International Journal of Design & Nature and Ecodynamics
Vol. 19, No. 5, October, 2024, pp. 1551-1561
Journal homepage: http://iieta.org/journals/ijdne

Estimating Soil Erosion in Al-Aubyth Valley Using Modern Techniques and the RUSLE Equation

Kamal A. Al-Qayyssi, Khalid Sabbar Mohammed*, Saadoun Zahir Al-Dulaimi, Muthana K. Al-Rawi, Ahmed Flayyih Fayyadh

Geography Department, College of Education for Humanities, University of Anbar, Anbar 31001, Iraq

Corresponding Author Email: ed.khalid.sabar@uoanbar.edu.iq

https://doi.org/10.18280/ijdne.190509

Received: 13 July 2024
Revised: 7 August 2024
Accepted: 15 August 2024
Available online: 29 October 2024

Keywords:
soil erosion, modern techniques, Al-aubyth valley, RUSLE equation

ABSTRACT

The research aims to employ modern techniques to calculate the soil erosion by estimating and calculating the data on which the (RUSLE) equation depends in the Al-aubyth valley basin within the borders of Anbar Governorate for the period (2002-2022) using modern techniques, as the study relied on the availability of climate, soil and topography data, and by adopting the interpretation and analysis of the visuals of Satellite (Landsat 9, 5). The study result showed an increase in the area of erosion occurring in the soil of the study area 30.8045 km^2 between 2002-2022 in the all erosion degrees. The reasons for the increase the erosion is attributed to the rise in temperature and lack of vegetation cover, decrease the amount of the rain, increase in evaporation in addition increase in the dust storms. As well as the increase in overgrazing operations and the region's influence on military operations, which led to an increase in disintegration of the soil surface and increased exposure to both water and wind erosion.

1. INTRODUCTION

The amount of eroded soil is considered an important environmental problem that affects all investments in arid and semi-arid areas, as the main cause of erosion is the dryness of the area, weak vegetation cover, and disintegration of the soil, which exposes it to water transport during the precipitation season and continuous wind transport most days of the year [1]. Therefore, estimating it is crucial to understanding the effects of this phenomenon on environmental sustainability [2].

To avoid risks, many mathematical models have been adopted that help predict the extent of erosion and determine the effectiveness of soil against wind and water erosion, including the Frouir equation. In this study, we have adopted the modified global equation model for soil erosion (RUSLE), as geographic information systems techniques and remote sensing visuals were used in the modeling. This equation and the production of digital maps achieve the required goals of calculating the areas affected by erosion and developing solutions to reduce the phenomenon of erosion and stabilize and preserve the soil as it is an irreplaceable natural resource [3]. Studying and measuring erosion is the first for the region, so estimating it is crucial to understanding the effects of this phenomenon. Environmental sustainability. The problem of erosion represents a challenge to many farmers and concerned institutions to avoid its negative effects, as failure to address this problem leads to many losses that cause damage to roads and infrastructure. The other is a decline in agricultural land areas. In addition to the problems, it causes to human health and various activities. The research focused on providing maps of soil and rainfall and adopting the necessary data in order to reach the desired goal.

1.1 Study problem

The research problem is embodied in employing geographic information systems techniques to model mathematical equations related to the phenomenon of soil erosion and estimate the amount of annual loss in tons/ha, which helps decision-makers predict erosion rates, which in turn helps in avoiding many risks before they occur, as well as diagnosing Points of danger and categorized according to severity to be treated in appropriate ways.

1.2 Study hypothesis

- There is soil erosion, especially in areas with steep slopes.
- Enabling modern technologies to give a clearer picture of the problem by analyzing visuals and producing maps showing the causes of drift.

1.3 Study objectives

The research aims to study and analyze the use of the global soil erosion equation in calculating the amount of eroded soil in the Al-aubyth valley basin, west of Anbar Governorate, and to identify erosion areas that pose a threat to the soil, as well as determining the impact of each erosion factor in the region through modern technologies. Providing results showing the effects of this phenomenon on the environment and local communities using available global data with sufficient accuracy, and producing digital maps of the factors affecting

soil erosion to give a clear picture of the problem.

1.4 Location of the study area

Al-aubyth valley basin, the second longest valley in Iraq after Horan valley, extends in western Iraq between Anbar and Karbala governorates. It flows for a distance of 297km towards the east, according to the direction of the main faults of the region, to empty into Al-Razzaza Lake at its southwestern edge, respectively. The Al-aubyth valley basin consists of Safawiyah Al-Sheikh valley, as well as the main branch of the valley, and its branches are distributed between Saudi and Iraqi lands (Figure 1). The area of the basin within the Iraqi border is 6538.47 km^2 [4]. What distinguishes the valley is that it is wide and deep with sloping edges, 1km wide and 40 to 50m deep. The walls of the valley are covered with stones and gravel, in addition to the areas surrounding it of hills and sand dunes. Although Al-aubyth valley basin is arid and dry, it is filled with seasonal troughs left by rainwater. The most famous of these troughs is Abu Maraji Water brook, located in the middle of the valley within Anbar Governorate. In some rainy years, the valley overflows with torrents that flow into Al-Razzaza Lake. The valley's spread out valleys, in addition to desert grasses and plants, provide good pastures for the Bedouins and their livestock (Figure 2) [5].

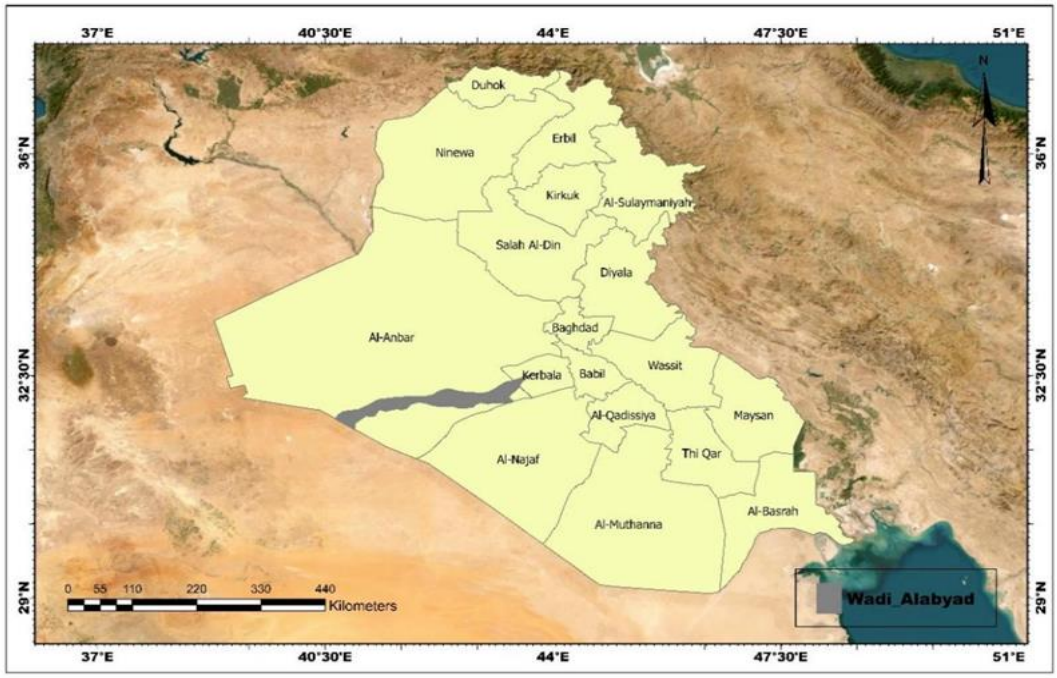

Figure 1. Study area
Source: Researchers' work based on Landsat visualizations using Arc map.

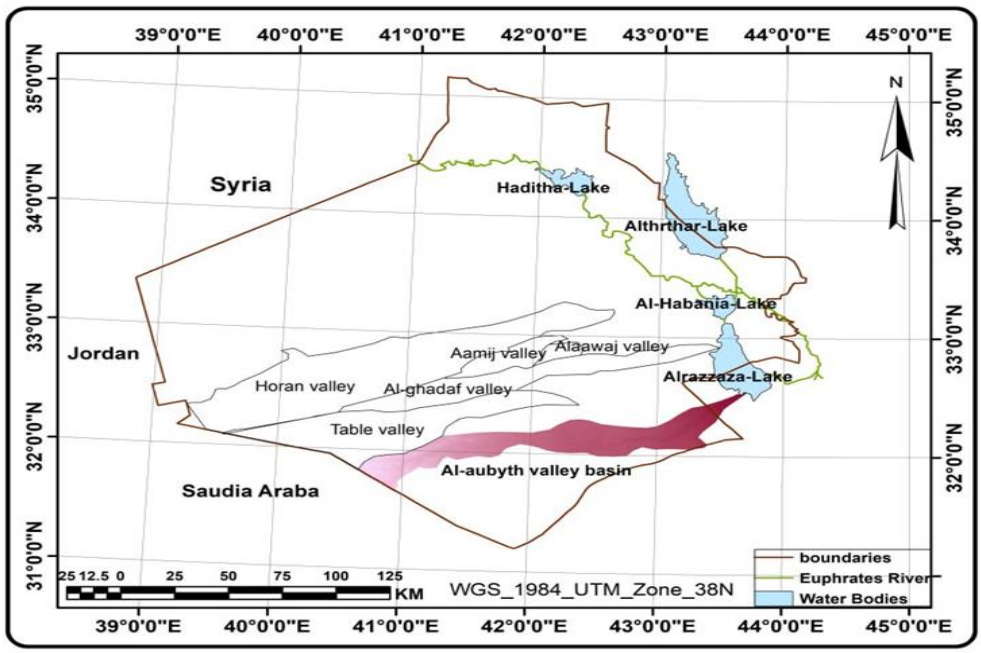

Figure 2. Some valleys in Anbar Governorate
Source: Republic of Iraq, Ministry of Water Resources, Directorate of Public Survey, Anbar Administrative Map, scale 500,000/1, 2012.

2. PHYSICAL CHARACTERISTICS

2.1 Geological properties

Tectonic movements during geological times had a varying impact on the region through the nature of the deposits and their stratigraphic succession. The rock excavations cover a period extending from the Upper Cretaceous period until the modern era. The stratigraphic succession begins with the Al-Tayarat Formation, which is the oldest rock unit that appears in the northwestern part of the region, about 10km east of the village of Medesis. It consists of lead-coloured dolomite rocks interspersed with recrystallized limestone and limestone, with a thin layer of red carbonitic clay at the top of the formation, and the age of the upper Cretaceous formation (Maastretitic) [6].

Above this formation is the Umm Ardhma Formation, which Al-Mubarak and Amin divided into two parts in 1983 based on the heterogeneity of rocks and the variation in fossils. The lower member dates back to the age of the Middle Pliocene, while the upper member dates back to the age of the Upper Pliocene, and the dividing line between them is indicated by a violet sandy limestone. It is topped with quartz sandstone. This formation is exposed within the study area between the two faults in the region (Mukht, Medicis), (Zirka, Usman). This is for the lower member and the upper part appears in the western part of the study area (Figure 1) [7].

The formation was deposited in a nitrite marine environment or a tidal or sub tidal environment, after which a marine retreat occurred that continued until the Eocene. After that, a new marine advance occurred that covered the area during this period, which led to the deposition of the Dammam Formation as a result of a marine advance in a nitrite shallow marine environment as well as a tidal and sub tidal environment [8].

The Dammam Formation is overlain by the Al-Zahra Formation, which appears in the eastern part of the study area. It is in the form of isolated longitudinal hills and consists of two units: the lower is a carbonic sandstone unit, and the upper is a thinly layered limestone unit these two layers were deposited in a transitional environment between marine and continental, and the age of this formation dates back to the middle Miocene era [9]. All of these formations are covered by sediments from the Quaternary era, which is the most recent unit of time and represents the last 1.88 million years of the Earth's life [10]. It is divided into two eras: from the oldest to the newest, the Pleistocene and the Holocene. Its deposits date back to these two periods, and it consists of from a mixture of gravel, sand, clay, and limestone rock fragments quaternary deposits are divided into [11]:

- Habaria Gravel.
- Terraces.
- Valley Filling.
- Rain Washed.
- Mass of Rock.
- Desert Plain Cover.

Valley-filling deposits represent gravel, sand, and mixed soil (loam) that are collected within the study area.

As for sediments washed away by rain water, they result from the process of washing the products and erosion of rocks and sediments that surround the site and which collect in depressions and shallow valleys. These sediments are mainly composed of mixed materials and small rock pieces consisting mainly of calcite, quartz, dolomite, and gypsum, and their average thickness is approximately 1-2 meters [12]. The rock pieces cover a large area of the desert surface near the stratigraphic detectors. They are of different sizes, ranging from several millimeters to large blocks. They are the result of mechanical weathering of the rock layers present in the region. They consist of two types:

(1) Ordinary rock pieces consisting of dolomite - crystalline limestone (Hamad phenomenon).

(2) Rock pieces covered with desert pigment and consisting of silicaugert (bed phenomenon).

Both of them are located within the eastern part of the study area (east of Faydat Al-Habbariyah), and were distinguished through satellite aerial photographs. The cover of the desert plains is formed as a result of the factors of fracture and decomposition of the various rocks present in the area. It is mainly made of salty clay materials with a dark coffee color and mixed with small pieces of rock. Its mineral content is calcite, quartz, clay minerals and gypsum, and its average thickness is 2m. It covers the rock layers. In most parts of the region [13].

As for slope deposits, they are considered one of the few or non-existent phenomena within the study area because their presence is associated with steep surfaces or deep-bottomed valleys.

Finally, the region is part of the Western Plateau, and the existing layers, that is, those mentioned in the geology of the region, are almost flat or have a very slight slope of (1-2) towards the east and southeast [14] (Figure 2).

2.2 Climate properties

The region is dominated by a dry desert climate, with moderate, humid, little rain in the winter, where the average rainfall is less than 75 millilitres, where the average rainy days do not exceed 40-60 days and even the rainy months from November to May, when the rain comes in the form of sporadic showers specifically. It is a torrential flood [15], and as it is known, it is the precipitation of the processes of erosion and sedimentation and the resulting geomorphological manifestations in terms of the selection of valleys, valleys, disparities, and other things, and the gathering of waterways and valleys sloping towards the lower slopes, and taking clear and easy areas as well [16]. The river breaks its course and the valley expands, and at the end of these processes flat plains are formed, expanding and expanding, which is the end of treatment and stability [17].

The climate of the study area, which is located in southwestern Iraq, was analyzed based on the monthly averages of climate coefficients from the Nukhayb climate station for the period from 2000-2024.

Temperatures affect the shapes of the Earth's surface as well as other climatic elements, and this effect appears through their role in mechanical and chemical weathering processes, and the processes of breakage, flaking, fragmentation, and reactions they cause [18].

Average temperatures during the day reach 20°C, while they reach 1°C during the night in the winter, and reach about 49°C in the summer. The average annual temperature is (10-12°C) in the winter and (22-24°C) in the winter. Spring, (32-34°C) in the summer, and (20-22°C) in the fall. As is known, temperature has an inverse relationship with rain and humidity and a direct relationship with wind. Temperatures increase during the months of July and August and decrease during the months of January and February [19].

2.3 Soil properties

The main research topic was to evaluate soil erosion rates for two time periods. Soils were classified into four categories:

Sandy, lime-mixed soil

These are soils that contain calcareous horizons. It is classified as a group of typical Calcites soils in the American system of soil classification, and a group of Calciyermosals in the FAO system. These soils consist of limestone rocks spread within the limestone formations of the Euphrates, and are often of medium depth, their depth not exceedingly more than (70 cm) or less, depending on their location. Geomorphologically, its color varies from light brown in the dry state to brown in the wet state. These soils have a weak lamellar structure in the upper horizons [20]. The texture of these soils is cohesive in the dry state and weak in the wet state. These soils are spread in the eastern parts of the study area can be seen in Figure 3.

Desert alluvial sedimentary soil

These soils belong to the newly formed (Enti-soils) soils in the modern American system (USDA 2010) and to the rank (Eutric Fluvisors) in the FAO system. These soils are undeveloped desert sedimentary soils called valley-filling soils that were collected as a result of erosion processes and washed away by flood waters from high areas. They are characterized by being of medium depth, not exceeding 50 cm. Their color varies from pale brown in its dry state to yellowish brown. yellowish brown in its wet state, these soils are weakly structured and loose. They are sediments of coarse to moderate coarseness and are unable to form and adhere. These soils are characterized by their levels of reaction being neutral to lightly basic, and with low salinity because they are washed soils. They are often formed in the form of longitudinal strips on both sides of the valley [21]. These soils are spread in the northwestern parts of the study area are seen in Figure 3.

Limestone-sandy mixture soil and limestone mixture soil

The soils of this group represent developed desert gypsum soils containing calcaid horizons and gypsids, and at the same time these soils are developed. The gypsum intersects at the bottom and the lime at the top, sometimes in the form of lumps. Adjoining to each other in a conglomerate form, the soils of this group are shallow in depth, characterized by varying color between reddish yellow in its dry state to dark brown (strong brown) in its wet state. The soils of this group are characterized by terraces of weak basic interaction and medium salinity in which the percentage of alternating Gypsum (calcium sulphate) with lime (calcium carbonate) [22]. These soils are spread throughout the northern and southern parts of the study area, as shown in Figure 3.

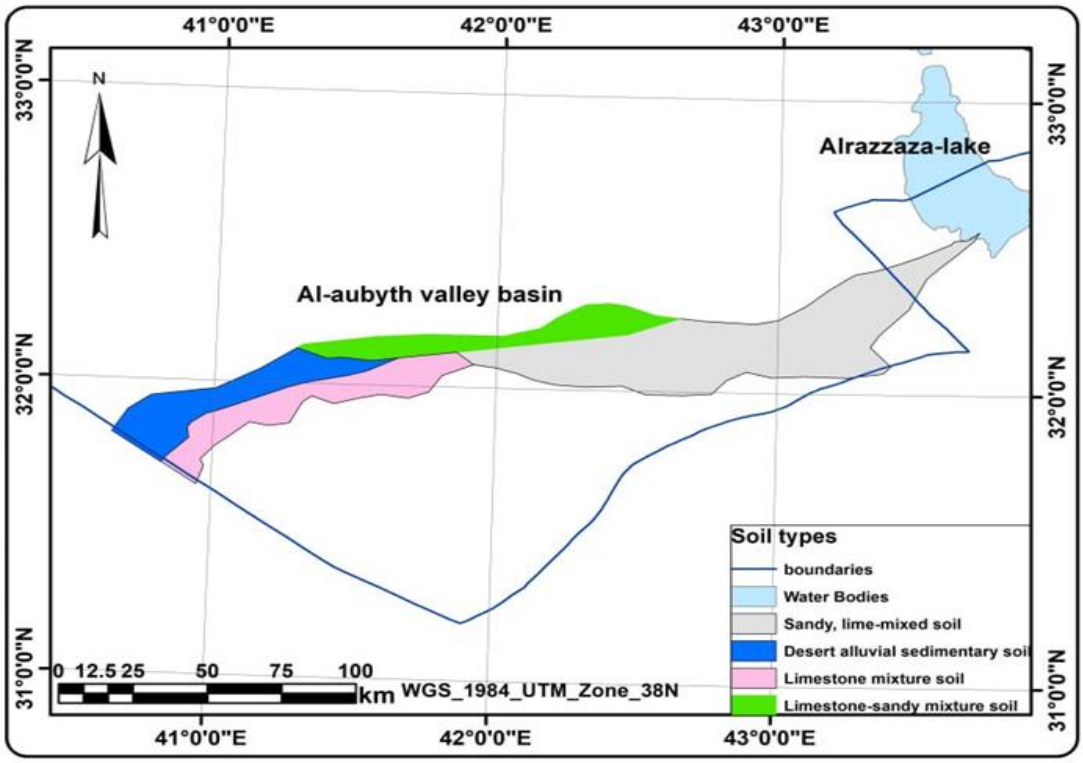

Figure 3. Soils types in study area
Source: Landsat satellite images by using ArcGIS 10.8.

3. METHODOLOGY

The study followed the descriptive analytical approach in achieving the objectives of the study, as it relied on the analysis of satellite images of the Landsat 5 and 9 satellites, which were obtained from the United States Geological Survey (USGS) website (https://earthexplorer.usgs.gov) as primary sources of data. As well as auxiliary data, reviewing previous studies and research that dealt with the global soil erosion equation, and analyzing the available data and information on the subject of the study, producing final maps that classified the study area into categories according to its susceptibility to the risk of erosion, and determined the value of each variable or parameter based on the information and

data extracted from its sources [23].

RUSLE equation helps the researchers to assess land degradation through soil related measures and RUSLE used to estimates long-term annual soil loss due to erosion across different land uses and land management activities. The Universal Soil Erosion Equation (RUSLE) was used also to estimate the amount of sediments in the Al-aubyth valley basin (within the Iraqi borders). The equation includes coefficients as shown below [24]:

$$A=R.\ K.\ LS.\ C.\ P$$

where,

A= Amount of soil washed away (tons/ha/year).

R= rain erosion factor, representing the surface portion of rainfall that causes soil erosion.

K= soil erodibility factor, which represents the geological and mechanical ability of the soil to resist erosion.

LS= slope length coefficient, representing the spatial effect of terrain on soil erosion.

C= Coefficient of effect of vegetation cover and land use on soil erosion.

P= Preservation or protection factor, practices used to reduce soil erosion.

The values of these coefficients can be calculated using the data. The values of the coefficients can then be multiplied together to obtain the final soil erosion value, where by the RUSLE when combined with RS and GIS, helps to identify the erosion-prone hotspots, predict the cell-by-cell soil erosion/loss, and prioritize the sub-watersheds in a big watershed in relation to the amount of soil loss from their catchments [25].

3.1 Data used

3.1.1 Digital elevation model (DEM)

6 digital images were obtained at different dates from the USGS website. A mosaic was created and then a projection process was performed to convert from WGS84 to the plane coordinate system UTM zone 38 N, so the cell size became 30 m after the projection process as illustrated in Figure 4.

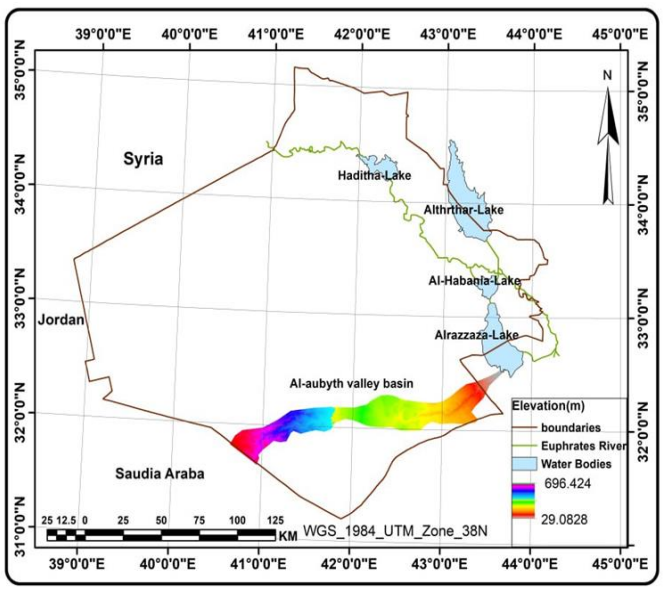

Figure 4. DEM of the study area

Source: Researchers' work based on Landsat visualizations using Arc map (10.8).

It represents a map of elevations in the study area, where the lowest point is 28.9 m above sea level, and the highest point is 696.4 m above sea level. It is known that the elevation factor plays an important role in the erosion process, as it depends on the degree of slope. And the slope, which increases the possibility of soil erosion occurring as a result of the clear gradient in elevation on Figure 4.

4. RESULT AND DISCUSSION

4.1 Slope degree factor (S)

Based on the digital elevation model, the (slope) was calculated in percentage. The values ranged from 2% to 48%, as the greater the value of the slope, the greater the possibility of soil erosion due to the tilt of the ground from the horizon, as it depends mainly on the slope of the surface, and to determine the value of the factor (S). The equation was applied [9]:

$$S=(0.43+0.30*slope+0.043*slope^2)/6.613$$

where,

S: Degree of slope.

Slope: Slope in percentage.

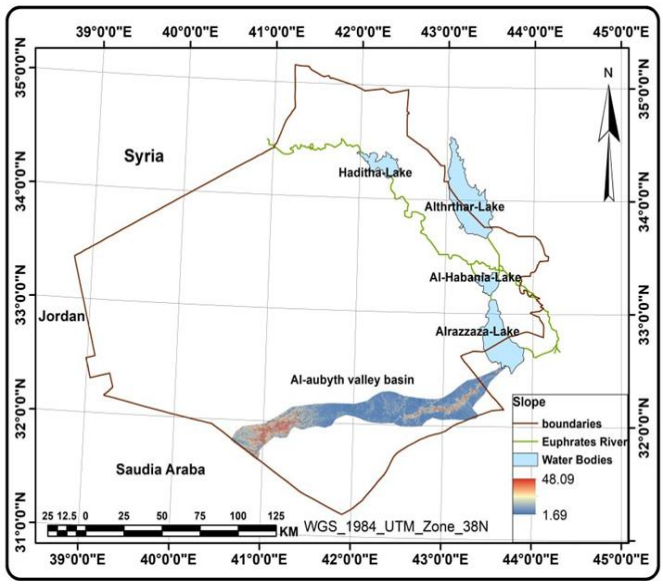

Figure 5. Spatial distribution of the S factor

Source: Researchers' work based on Landsat visualizations using Arc map.

This factor is considered one of the most important factors involved in the erosion process, as the amount of erosion is directly proportional to the degree and direction of the slope, and thus the total erosion of the soil increases with the increase in the length of the slope. Depending on the above equation, the degree of slope was distributed in a range (1.69-48.09%), and the degrees of slope can be divided into Al-aubyth valley basin [26], as shown in Figure 5.

4.2 Slope length factor (L)

The length of the slope affects soil erosion by giving sufficient time for the soil dismantling and erosion processes, and the probability of erosion increases with the increase in the value of the factor L. The following equation was used to

estimate the effect of this factor [27]:

$$L=\{(A^{1.4})-(B^{1.4})\}/\{\text{Cell size}*(22.14^{0.4})\}$$

where,

Cell size: The spatial resolution of the digital elevation model is 30 meters.

B= Flow accumulation.

A= B + cell size/cell size (pixels).

By applying the previous equation, we found that the values of the parameter L, which are represented in Figure 6:

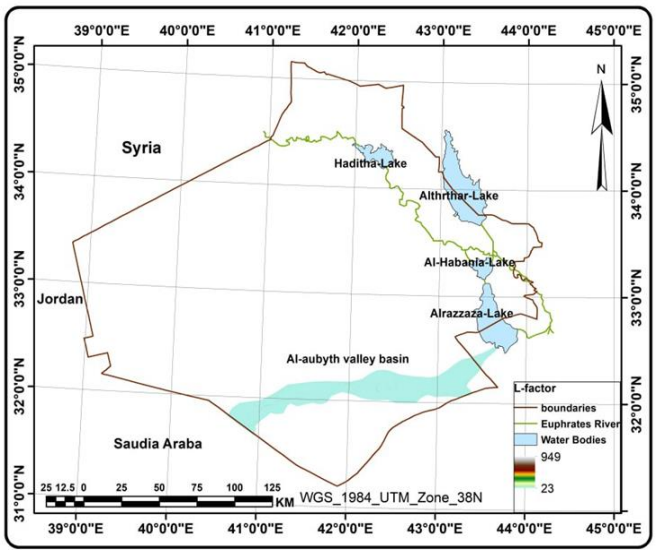

Figure 6. Spatial distribution of the factor (L)
Source: Researchers' work based on Landsat visualizations using Arc map.

The highest value was recorded in steep areas, while the lowest effect of this factor was recorded in flat and semi-flat areas with a low slope spread throughout the region and the plains [28] in Figure 6.

4.3 Rainfall factor (R) (2002-2022)

It is the factor influencing the process of soil erosion through the influence of raindrops on the scattering and separation of soil particles, as well as the increase in the amount of soil washed away with an increase in rainfall. For the purpose of estimating this factor, it is possible to obtain rainfall values during the study period from the PERSIANN system [29]. Operational from (https://chrsdata.eng.uci.edu/). It is one of the most widely used mathematical models to estimate soil erosion due to water. The PERSIANN algorithm used here relies on geostationary long wave infrared images to generate global rainfall.

Figure 7 represented from Figures 5 and 6, the annual rainfall rate in mm/year, noting that the rainfall rate in 2022 has increased over the year 2002. Due to the unavailability of rainfall data in the study area, the average annual rainfall was used to calculate the R factor through the following equation [30].

$$R=0.0483*(P^{1.610})$$

where,

R= Rainfall factor.

P= The annual rainfall rate estimated in mm/year.

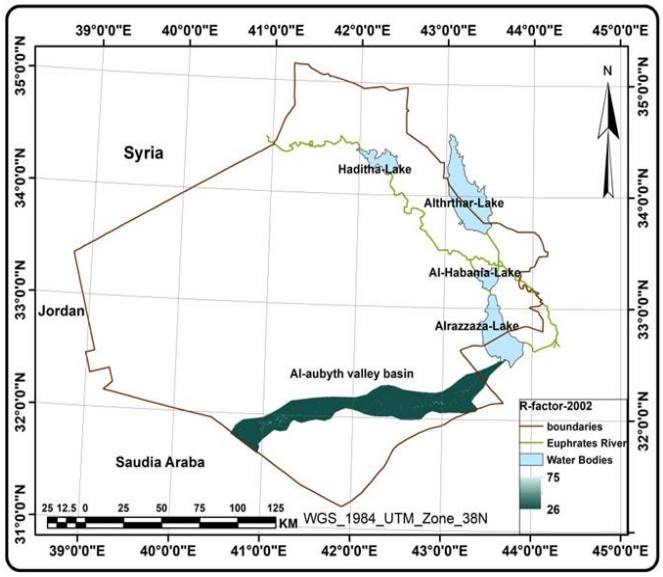

Figure 7. Amount of rainfall (mm/year) in the study area (2002)
Source: Researchers' work based on Landsat visualizations using Arc map (10.8).

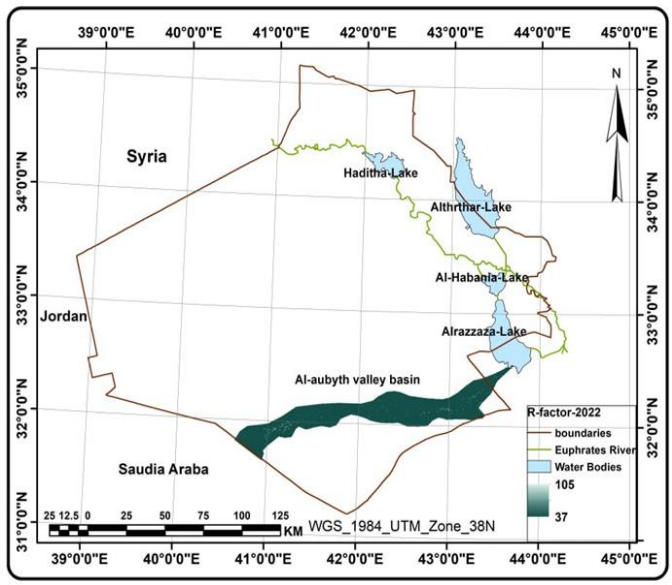

Figure 8. Spatial distribution of rain erosion factor (R) (2022)
Source: Researchers' work based on Landsat visualizations using Arc map (10.8).

The rain erosion R were calculated and the values were distributed in a range of (75_26)(105_37)mm/year, as shown in Figure 8 respectively. It is clear that the minimum values of the R factor are located in the western part of the study area, while the highest value can be observed in the eastern part of the region [31].

4.4 Vegetation factor (C)

It is known as the vegetation coefficient, as soil erosion is affected by vegetation cover by reducing the intensity of surface runoff. If the surface contains vegetation cover, the resistance of the soil to erosion will be higher, but if the ground is fallow and does not contain any type of vegetation cover, it will be more affected. By erosion, and its resistance is less, especially if other factors combine, such as: intense rain and

steep slope. Based on the NDVI guide, which was calculated according to the equation [32].

$$NDVI=(NIR-Red)/(NIR+Red)$$

Since,

NIR = Reflectivity of red rays.

Red = Reflectivity of blue rays.

whereas, NDVI is the natural coefficient of variation of vegetation cover.

The value of C was calculated according to the following equation [33]:

$$C=0.431-0.805*NDVI$$

After implementing the equation, a map was derived that represents the effect of vegetation cover on soil erosion in the study area (Figures 9 and 10).

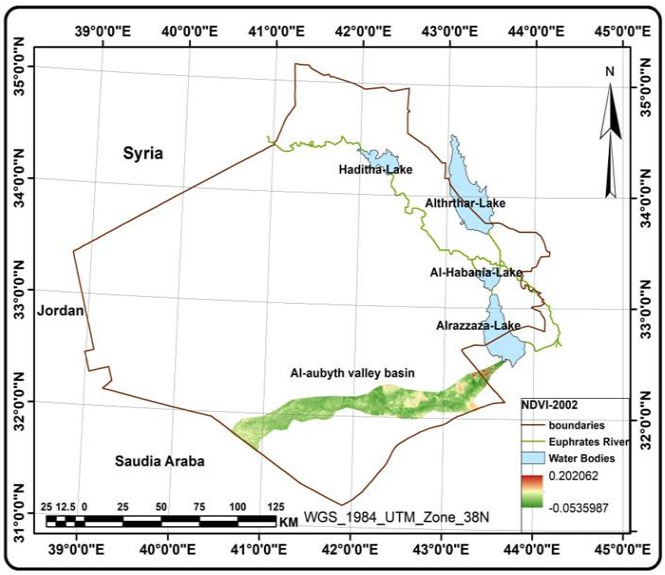

Figure 9. NDVI values in the study area (2002)
Source: Researchers' work based on Landsat visualizations using Arc map (10.8).

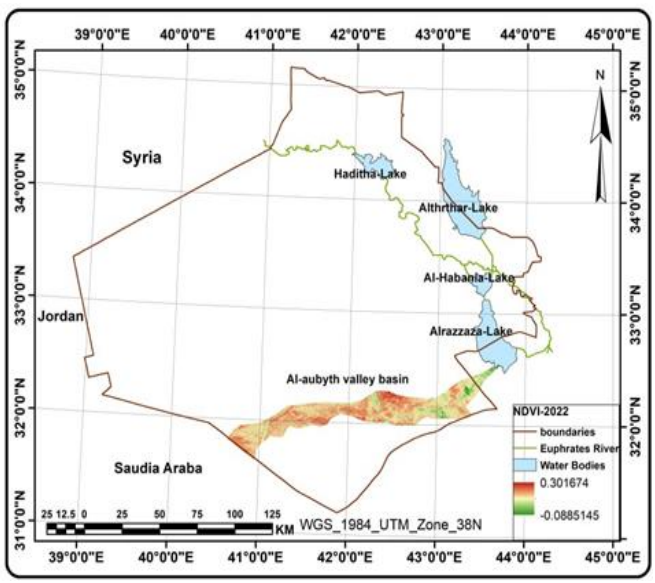

Figure 10. NDVI values in the study area (2022)
Source: Researchers' work based on Landsat visualizations using Arc map (10.8).

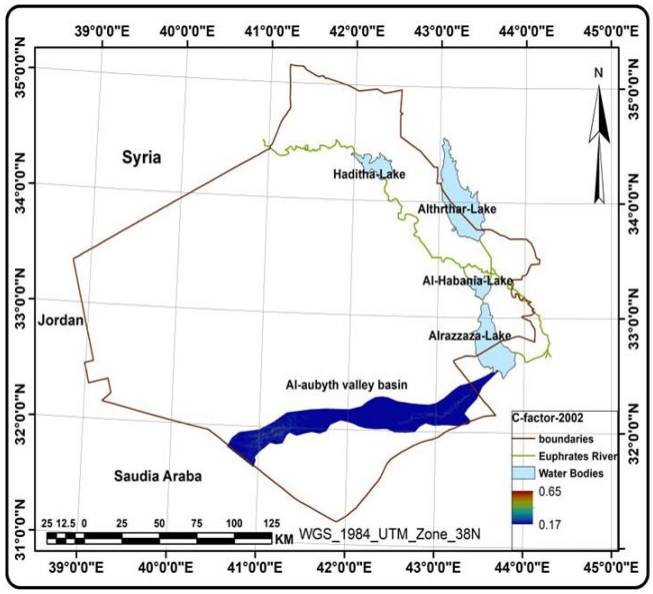

Figure 11. Spatial distribution of vegetation factor (C) (2002)
Source: Researchers' work based on Landsat visualizations using Arc map (10.8).

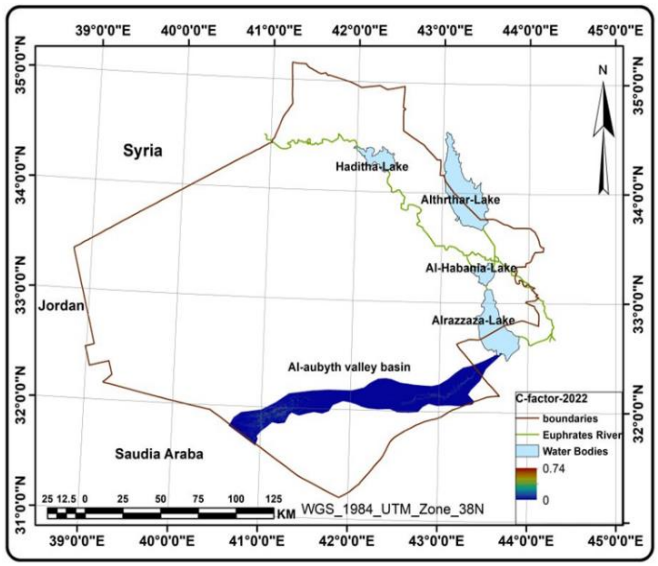

Figure 12. Spatial distribution of vegetation factor (C) (2022)
Source: Researchers' work based on Landsat visualizations using Arc map (10.8).

The NDVI vegetation index is used to highlight vegetation cover, as NDVI values range from -1 to +1 and positive results indicate that the cell has vegetation cover, and vice versa. From Figures 9 and 10, it is evident that the values of vegetation density (NDVI) vary during the study period [34], as the value of NDVI increased in 2022 than it was in 2002, due to the increase in human activity and the intensity of rain, in addition to the security events that the region witnessed, which led to a decline in areas covered by vegetation in the study area. And for the purpose of showing the value of the coefficient C by applying the equation, it becomes clear to us that the values of the coefficient C were distributed in a range of (0-65_0-17) in the year 2002 and in a range of (0-74_0) in the year 2022, as shown in Figures 11 and 12.

It is clear that there is an inverse relationship with the value

of the vegetation index in the region, as areas with a low NDVI value take a high value of the C factor, and cultivated areas take a low value of the C factor [35].

4.5 Crop management factor (P)

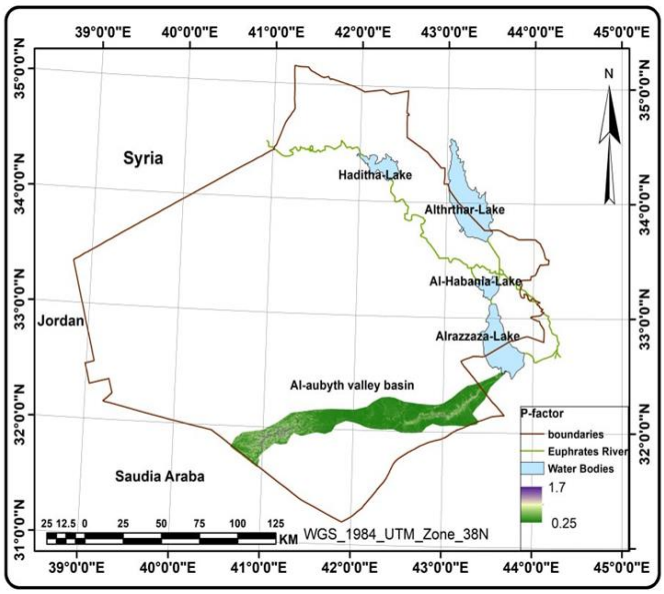

Figure 13. Spatial distribution of crop management factor (P)
Source: Researchers' work based on Landsat visualizations using Arc map (10.8).

The P factor expresses the measures used to reduce soil erosion, such as growing plant barriers, curves, and reducing soil loss in a specific location, in addition to reducing the effect of the slope factor. Depending on the values of the slope of the land, its value ranges between 1-0, and high values of this factor indicate a lack of maintenance measures. Soil To reduce soil erosion, the values of the coefficient (P) were calculated according to the equation [36]:

$$P=0.2+0.03*Slope$$

The value of the index increases with the increase in the value of the Earth's inclination from the horizon, as the values are distributed in a range (0.2_1.7), and the steep areas take the highest values of the P factor. Through analyzing the visuals used for the study area. The measures to preserve the soil from erosion are not at a good level except in some areas of the study area, which represent the center and east of the study area as shown in Figure 13 [37].

4.6 Soil erosion factor (K)

The researcher classified the soil based on the soil map produced by the Anbar Governorate Agriculture Directorate, and it was into four types. The study area covers Table 1, as this factor is considered one of the main factors that affect soil erosion. Through it, we can know the properties of the soil and estimate its susceptibility. Soil erosion, by finding the percentages of sand, silt and clay, in addition to knowing the permeability and structure of the soil [38]. Using GIS, a map of the eroded soil of the study area was created as shown in Figure 14 and Table 1.

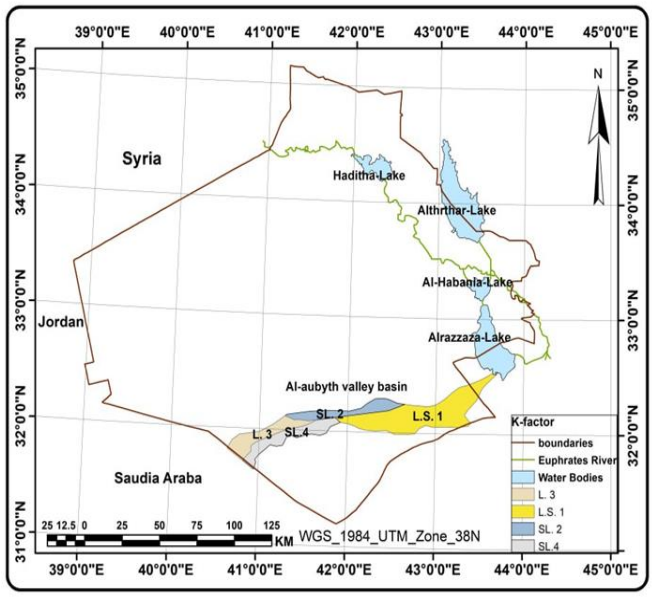

Figure 14. Eroded soil types in the study area factor (K)
Source: Researchers' work based on Landsat visualizations using Arc map (10.8).

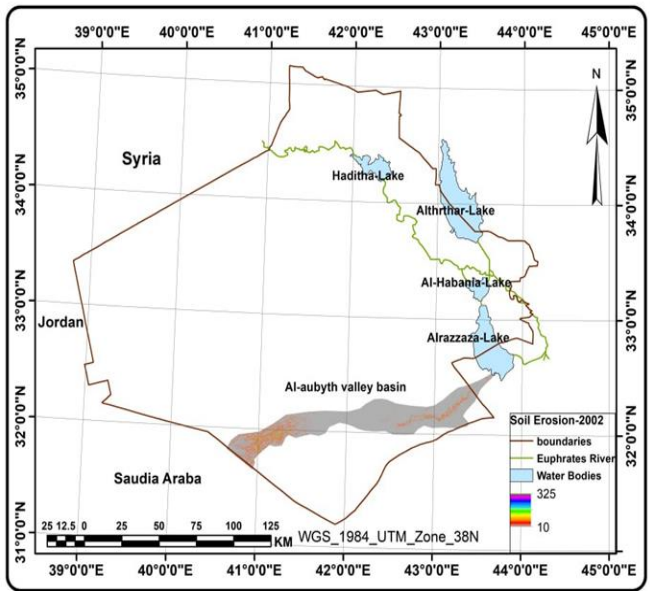

Figure 15. Spatial distribution of minimum and maximum soil loss
Source: Researchers' work based on Landsat visualizations using Arc map (10.8).

It is clear from Figure 15 and Tables 1 and 2 that there is an increase in the percentage of sand over the rest of the soil particles, as it was distributed in a range of (736-390) grams, kg, soil. While the percentage of silt was distributed in a range of (410-112) grams, kg, soil. As for clay, it was distributed in a range of (122-200) gm, kg, soil. The soil texture of the study area is characterized by its medium to moderate roughness, distributed between its mixed texture to its sandy mixed texture and its mixed sandy texture. In terms of chemical soil characteristics, it became clear that the soil of the study area is calcareous and gypsum, distributed on the plateaus, while desert sedimentary soil is located within the valley's stream and terraces [39].

Table 1. Description and classification of soils in the study area

Gross Soil Aggregate According to USDA Classification	Gypsum. Gm, kg, soil	Total Carbonate, gm, kg	Prophetic Distribution of the Volume of Losses from the Soil				Medium Depth	Site Number
			Soil Texture	Clay, gm, kg	Alluvial, gm, kg	Sand, gm, kg		
Calcareous soil	92	264	LS	152	112	736	30-0	1
Calcareous soil	97	287	SL	148	153	699	30-0	2
Desert sedimentary soil	103	238	L	200	410	390	30-0	3
Gypsum-limestone soil	204	258	SL	122	310	568	30-0	4

Source: Researchers' work based on the results of the visualizations.

Table 2. Soil erosion rates between 2002-2022

Category	Value of Soil Erosion	2002	2022	Amount of Variance
weak	10	6475.691	6492.12	16.429
middle	20	28.60436	39.75272	11.1483
high	50	13.20201	15.25566	2.0536
very high	100	3.227158	5.574182	2.34702
Severe erosion	>200	1.320201	2.200335	0.88013
total area (km^2)		6522.473	6552.702	**30.8045 km^2**

Source: Researchers' work based on the results of the visualizations.

5. CONCLUSIONS

1) The results showed that the process of soil erosion is a complex process that depends on several factors that are overlapping in their influence and that one cannot be separated from the other.

2) The results showed the possibility of adopting geospatial technologies to accurately monitor and follow the phenomenon of soil erosion, which saves time, effort and costs.

3) The results of the research proved that the slope factor (S) greatly affects the amount of eroded soil as the greater the slope value, the greater the possibility of erosion occurring in the soil due to the tilt of the earth from the horizon. The amount of erosion is directly proportional to the degree and direction of the slope.

4) The results of the research showed, according to the factor (L), that the amount of eroded soil increases with increasing slope length, which greatly affects the amount of eroded soil.

5) By analyzing the soil maintenance coefficient (P) unfortunately, it was found that the procedures to preserve the soil from erosion are not at a good level due to the weakness of government measures to reduce the phenomenon of soil erosion, except in some areas of the study area, which represent the center and east of the study area.

6) The results of the research showed the value of NDVI increased in 2022 than it was in 2002, due to the increase in human activity and the intensity of rain, in addition to the security events that the region witnessed, which led to a decline in areas Covered by vegetation in the study area.

Recommendations

1) Expanding the horizons of this research in following up and monitoring cases of erosion and monitoring dust storms and their negative effects.

2) Adopting sound administrative methods for managing soil in arid and semi-arid areas and preserving and building soil during use through the use of conservation agricultural methods and zero-sum agriculture.

3) Paying attention to developing vegetation cover to protect the soil from erosion.

REFERENCES

[1] Haregeweyn, N., Tsunekawa, A., Nyssen, J., Poesen, J., Tsubo, M., Tsegaye Meshesha, D., Schütt, B., Adgo, E., Tegegne, F. (2015). Soil erosion and conservation in Ethiopia: A review. Progress in Physical Geography, 39(6): 750-774. https://doi.org/10.1177/0309133315598725

[2] Lal, R. (1993). Soil erosion and conservation in West Africa. World Soil Erosion and Conservation, 7-25. https://doi.org/10.1017/CBO9780511735394.003

[3] Rostagno, C.M., Degorgue, G. (2011). Desert pavements as indicators of soil erosion on aridic soils in north-east Patagonia (Argentina). Geomorphology, 134(3-4): 224-231. https://doi.org/10.1016/j.geomorph.2011.06.031

[4] Labib, T.M. (1981). Soil erosion and total denudation due to flash floods in the Egyptian eastern desert. Journal of Arid Environments, 4(3): 191-202. https://doi.org/10.1016/S0140-1963(18)31560-X

[5] Dunkerley, D.L., Brown, K.J. (1997). Desert soils. Arid Zone Geomorphology: Process, Form and Change in Drylands, 55-68. https://doi.org/10.1016/B978-0-444-89198-3.50015-5

[6] Breckle, S.W., Veste, M., Wucherer, W. (2001). Deserts, land use and desertification. In Sustainable Land Use in Deserts. Springer Berlin Heidelberg, pp. 3-13. https://doi.org/10.1007/978-3-642-59560-8_1

[7] Jeong, A., Dorn, R.I., Seong, Y.B., Yu, B.Y. (2021). Acceleration of soil erosion by different land uses in arid lands above 10Be natural background rates: Case study in the Sonoran Desert, USA. Land, 10(8): 834. https://doi.org/10.3390/land10080834

[8] Wainwright, J., Parsons, A.J., Abrahams, A.D. (1995). A simulation study of the role of raindrop erosion in the formation of desert pavements. Earth Surface Processes and Landforms, 20(3): 277-291. https://doi.org/10.1002/esp.3290200308

[9] Ludwig, J.A., Muldavin, E., Blanche, K.R. (2000). Vegetation change and surface erosion in desert grasslands of Otero Mesa, southern New Mexico: 1982 to 1995. The American Midland Naturalist, 144(2): 273-

285. https://doi.org/10.1674/0003-0031(2000)144[0273:VCASEI]2.0.CO;2
[10] Akuja, T., Avni, Y., Zaady, E., Gutterman, Y. (2001). Soil erosion effects as indicators of desertification processes in the northern Negev Desert. In Soil Erosion. American Society of Agricultural and Biological Engineers, pp. 595-598. https://doi.org/10.13031/2013.4847
[11] Lane, L.J., Kidwell, M.R. (2003). Hydrology and soil erosion. Santa Rita Experimental Range, 100: 1903-2003.
[12] Buckhouse, J.C., Mattison, J.L. (1980). Potential soil erosion of selected habitat types in the high desert region of central Oregon. Rangeland Ecology & Management/Journal of Range Management Archives, 33(4): 282-285.
[13] Labib, T.M. (1981). Soil erosion and total denudation due to flash floods in the Egyptian eastern desert. Journal of Arid Environments, 4(3): 191-202. https://doi.org/10.1016/S0140-1963(18)31560-X
[14] Maltsev, K., Yermolaev, O. (2020). Assessment of soil loss by water erosion in small river basins in Russia. Catena, 195: 104726. https://doi.org/10.1016/j.catena.2020.104726
[15] Mohammad, K.S., Samat, N., Khalid, H.N. (2011). Using remote sensing and GIS for observation land use land cover changes and quantifying arable land loss in Penang Island - A case study of Balik Pulau. In 32nd Asian Conference on Remote Sensing 2011, pp. 1697-1715.
[16] Zhang, W., Zhou, J., Feng, G., Weindorf, D.C., Hu, G., Sheng, J. (2015). Characteristics of water erosion and conservation practice in arid regions of Central Asia: Xinjiang, China as an example. International Soil and Water Conservation Research, 3(2): 97-111. https://doi.org/10.1016/j.iswcr.2015.06.002
[17] Nearing, M.A., Simanton, J.R., Norton, L.D., Bulygin, S.J., Stone, J. (1999). Soil erosion by surface water flow on a stony, semiarid hillslope. Earth Surface Processes and Landforms: The Journal of the British Geomorphological Research Group, 24(8): 677-686. https://doi.org/10.1002/(SICI)1096-9837(199908)24:8%3C677::AID-ESP981%3E3.0.CO;2-1
[18] Poesen, J.W., Torri, D., Bunte, K. (1994). Effects of rock fragments on soil erosion by water at different spatial scales: A review. Catena, 23(1-2): 141-166. https://doi.org/10.1016/0341-8162(94)90058-2
[19] Du, H., Dou, S., Deng, X., Xue, X., Wang, T. (2016). Assessment of wind and water erosion risk in the watershed of the Ningxia-Inner Mongolia Reach of the Yellow River, China. Ecological Indicators, 67: 117-131. https://doi.org/10.1016/j.ecolind.2016.02.042
[20] Liu, B., Xie, Y., Li, Z., Liang, Y., Zhang, W., Fu, S., Yin, S., Wei, X., Zhang, K., Wang, Z., Liu, Y., Zhao, Y., Guo, Q. (2020). The assessment of soil loss by water erosion in China. International Soil and Water Conservation Research, 8(4): 430-439. https://doi.org/10.1016/j.iswcr.2020.07.002
[21] Gyssels, G., Poesen, J., Bochet, E., Li, Y. (2005). Impact of plant roots on the resistance of soils to erosion by water: A review. Progress in Physical Geography, 29(2): 189-217. https://doi.org/10.1191/0309133305pp443ra
[22] Almasalmeh, O., Saleh, A.A., Mourad, K.A. (2022). Soil erosion and sediment transport modelling using hydrological models and remote sensing techniques in Wadi Billi, Egypt. Modeling Earth Systems and Environment, 8(1): 1215-1226. https://doi.org/10.1007/s40808-021-01144-1
[23] Yang, J.L., Zhang, G.L., Yang, F., Yang, R.M., Yi, C., Li, D.C., Zhao, Y.G., Liu, F. (2016). Controlling effects of surface crusts on water infiltration in an arid desert area of Northwest China. Journal of Soils and Sediments, 16: 2408-2418. https://doi.org/10.1007/s11368-016-1436-z
[24] Jiang, C., Zhang, H., Zhang, Z., Wang, D. (2019). Model-based assessment soil loss by wind and water erosion in China's Loess Plateau: Dynamic change, conservation effectiveness, and strategies for sustainable restoration. Global and Planetary Change, 172: 396-413. https://doi.org/10.1016/j.gloplacha.2018.11.002
[25] Wassif, M.M., Wassif, O.M. (2021). Sustainable soil management to mitigate soil erosion hazards in Egypt. In: Management and Development of Agricultural and Natural Resources in Egypt's Desert, pp. 163-211. https://doi.org/10.1007/978-3-030-73161-8_7
[26] Prasannakumar, V., Vijith, H., Abinod, S., Geetha, N.J.G.F. (2012). Estimation of soil erosion risk within a small mountainous sub-watershed in Kerala, India, using revised universal soil loss equation (RUSLE) and geo-information technology. Geoscience Frontiers, 3(2): 209-215. https://doi.org/10.1016/j.gsf.2011.11.003
[27] Mukanov, Y., Chen, Y., Baisholanov, S., Amanambu, A.C., Issanova, G., Abenova, A., Fang, G., Abayev, N. (2019). Estimation of annual average soil loss using the revised universal soil loss equation (RUSLE) integrated in a geographical information system (GIS) of the esil river basin (ERB), Kazakhstan. Acta Geophysica, 67: 921-938. https://doi.org/10.1007/s11600-019-00288-0
[28] Karthick, P., Lakshumanan, C., Ramki, P. (2017). Estimation of soil erosion vulnerability in Perambalur Taluk, Tamilnadu using revised universal soil loss equation model (RUSLE) and geo information technology. International Research Journal of Earth Sciences, 5(8): 8-14.
[29] Lane, L.J., Renard, K.G., Foster, G.R., Laflen, J.M. (1992). Development and application of modern soil erosion prediction technology-The USDA experience. Soil Research, 30(6): 893-912. https://doi.org/10.1071/SR9920893
[30] Farhan, Y., Nawaiseh, S. (2015). Spatial assessment of soil erosion risk using RUSLE and GIS techniques. Environmental Earth Sciences, 74: 4649-4669. https://doi.org/10.1007/s12665-015-4430-7
[31] Ganasri, B.P., Ramesh, H. (2016). Assessment of soil erosion by RUSLE model using remote sensing and GIS-A case study of Nethravathi Basin. Geoscience Frontiers, 7(6): 953-961. https://doi.org/10.1016/j.gsf.2015.10.007
[32] Biswas, S.S., Pani, P. (2015). Estimation of soil erosion using RUSLE and GIS techniques: A case study of Barakar River basin, Jharkhand, India. Modeling Earth Systems and Environment, 1: 1-13. https://doi.org/10.1007/s40808-015-0040-3
[33] Papaiordanidis, S., Gitas, I.Z., Katagis, T. (2019). Soil erosion prediction using the Revised Universal Soil Loss Equation (RUSLE) in Google Earth Engine (GEE) cloud-based platform. Бюллетень Почвенного института им. ВВ Докучаева, (100): 36-52.
[34] Ozsoy, G., Aksoy, E., Dirim, M.S., Tumsavas, Z. (2012).

Determination of soil erosion risk in the mustafakemalpasa river basin, turkey, using the revised universal soil loss equation, geographic information system, and remote sensing. Environmental Management, 50: 679-694. https://doi.org/10.1007/s00267-012-9904-8

[35] Lee, E., Ahn, S., Im, S. (2017). Estimation of soil erosion rate in the Democratic People's Republic of Korea using the RUSLE model. Forest Science and Technology, 13(3): 100-108. https://doi.org/10.1080/21580103.2017.1341435

[36] Imamoglu, A., Dengiz, O. (2017). Determination of soil erosion risk using RUSLE model and soil organic carbon loss in Alaca catchment (Central Black Sea region, Turkey). Rendiconti Lincei, 28: 11-23. https://doi.org/10.1007/s12210-016-0556-0

[37] Millward, A.A., Mersey, J.E. (1999). Adapting the RUSLE to model soil erosion potential in a mountainous tropical watershed. Catena, 38(2): 109-129. https://doi.org/10.1016/S0341-8162(99)00067-3

[38] Markose, V.J., Jayappa, K.S. (2016). Soil loss estimation and prioritization of sub-watersheds of Kali River basin, Karnataka, India, using RUSLE and GIS. Environmental Monitoring and Assessment, 188: 1-16. https://doi.org/10.1007/s10661-016-5218-2

[39] Egbueri, J.C., Igwe, O., Ifediegwu, S.I. (2022). Erosion risk mapping of Anambra State in southeastern Nigeria: Soil loss estimation by RUSLE model and geoinformatics. Bulletin of Engineering Geology and the Environment, 81(3): 91. https://doi.org/10.1007/s10064-022-02589-z